Check for updates

Remarkably selective biocompatible turn-on fluorescent probe for detection of Fe^{3+} in human blood samples and cells†

Vishaka V. H.,[a] Manav Saxena, [iD][a] Geetha Balakrishna R., [iD]*[a] Sachin Latiyan[bc] and Shilpee Jain[c]

The robust nature of a biocompatible fluorescent probe is demonstrated, by its detection of Fe^{3+} even after repeated rounds of quenching (reversibility) by acetate in real human blood samples and cells *in vitro*. Significantly trace levels of Fe^{3+} ions up to 8.2 nM could be detected, remaining unaffected by the existence of various other metal ions. The obtained results are validated by AAS and ICP-OES methods. A portable test strip is also fabricated for quick on field detection of Fe^{3+}. As iron is a ubiquitous metal in cells and plays a prominent role in biological processes, the use of this probe to image Fe^{3+} in cells is a substantial development towards biosensing. Cytotoxicity studies also proved the nontoxic nature of this probe.

1. Introduction

Over the past few decades, traditional techniques like atomic absorption spectroscopy (AAS), inductively coupled plasma atomic emission spectroscopy (ICP-OES) voltammetry and colorimetric techniques[1] have been used for the detection of Fe^{3+}. Nonetheless, these techniques require advanced equipment, tiresome sample preparation procedures and trained professionals. Fluorescence techniques have been extensively applied by research groups to avoid these disadvantages. A number of fluorescent probes for selective sensing of Fe^{3+} ion have been developed.[2] As Fe^{3+} possesses paramagnetic nature in its 3d orbital it leads to fluorescence quenching.[3] Most of the early reported probes exhibited turn-off (fluorescence quenching) response because of the paramagnetic nature of Fe^{3+} ion that restricts its application in biological systems.[4] Turn on signals are dominant in biosensing compared to turn-off ones because of their good processing of signals in biological media.[5]

Highly optically active metal chalcogenide/quantum dots (QDs) have been reported as fluorescence based sensors/ receptors with excellent stability and photophysical properties.[6] Due to their tunable optical properties[6a,7] they have gained importance in numerous fields such as photovoltaics,[8]

bioimaging[9] and as sensors.[10,11] In the early years Jiang *et al.* reported a gallic acid modified nanometer sized alumina microcolumn separations and were able to detect up to 52.1 μM Fe^{3+} in real water samples using ICP-MS.[12] With time, in 2019 Mohammadi *et al.* developed a MBTBA-Fe_3O_4@SiO_2 nanocomposite fluorescent ligand capable of sensing Fe^{3+} with a detection limit of 43.09 nM.[13] Further Nibu *et al.* reported a dual responsive colorimetric/fluorescent turn-on sensor with detection limit up to 7.49 μM concentration.[14] All these probes were for iron detection in water samples. Reports on detection of metal ions other than Fe^{3+} in blood samples can also be found. In 2009 Jung *et al.* reported a BODIPY-functionalized magnetic silica nanoparticle fluorescent receptor for probing Pb^{2+} in children's blood[15] and the same group in 2010 reported a nitrobenzene-functionalized Ni@SiO_2 core/shell magnetic nanoparticles as a fluorogenic chemosensor that removed about 96% of Cu^{2+} in human blood.[16] Subsequently in 2011 a macrocyclic dioxotetraamine probe of two-photon excited chemosensor was designed by Liu *et al.* for determination of copper ions with a detection limit of 0.007 μM in human blood serum samples[17] based on the principle of ICT. Bandyopadhyay *et al.* reported a fluorescent ligand to determine the concentration of inorganic phosphate and detected about 1.82 mM of phosphate in chicken serum.[18] Recently, Vishaka *et al.* designed a colorimetric chemosensor for the sensing of Cu^{2+} with a detection limit of 1.31 μM in human blood serum samples.[19] For the first time in 2016 Wei *et al.* reported a Fe_3O_4@ZnO based fluorescent chemosensor for the detection of Fe^{3+} in human blood serum samples with 92.6–108.4% recovery[20] and no reports since then have been reported for such chemosensing of Fe^{3+} in blood. Interference of other transition metal ions, like Al^{3+}, Pb^{2+}, Hg^{2+}, Cu^{2+} with Fe^{3+} results in poor selectivity and

[a]*Center for Nano and Material Science, Jain University, Jakkasandra Post, Bangalore Rural-562112, India. E-mail: br.geetha@jainuniversity.ac.in*

[b]*Metallurgical and Materials Engineering, National Institute of Technology, Tiruchirapalli-620015, India*

[c]*Centre for Biosystems Science and Engineering, Indian Institute of Science, Bangalore-560012, India*

sensitivity of the chemosensor.[21] However many colorimetric and fluorometric chemosensors are described in the literature for intracellular imaging of cells.[22] Most of the reported probes cannot be used in live cells due to their cellular toxicity and many of them are susceptible to be affected by the background fluorescence since they possess a shorter emission wavelength below 550 nm.

Xanthene and its derivatives[23] with their spirocyclic structure being responsible for off and on fluorescence when the specific ion unbinds and binds to the probe respectively have been reported for detection of Fe^{3+} ions in water samples based on this mechanism.[24,25] Still most of the reported probes show some fragility and insufficiency like interference of other metal ions and poor sensitivity.[26] However, the present work on such probes for Fe^{3+} detection in human blood samples is first of its kind. Turn-on fluorescent probes favor high selectivity, sensitivity and anti-interference, hence it demands the synthesis of new fluorescent probes for the detection of Fe^{3+} ions.[27] Herewith, we report an excellent biocompatible rhodamine 6G-derivative fluorescent probe named **RG5NC** as a turn-on fluorescent sensor with high selectivity and sensitivity (in nM range) towards Fe^{3+} in the existence of various other metal ions. The probe exhibited negligible cytotoxicity.

2. Experimental

The materials and methods used for synthesis of probe (**RG5NC**) and its Fe^{3+} complex can be found in ESI 1–9,† wherein Schemes 1 and 2† explains the reactions involved. Details of preparation of stock solution for spectral determination, absorption and emission studies are explained in ESI 10 and 11.†

2.1 Detection of Fe^{3+} in real samples and human blood samples

Industrial waste water was collected from paper and plastic industry from Harohalli Industrial Area, Bangalore rural, Karnataka, India. Human blood samples were collected from Arunodaya Polyclinic, Harohalli, Bangalore and samples were digested as per the established standard protocol[28] and the obtained blood serum was used for further studies. Details of the certified reference material is attached in ESI 12.†

2.2 Cell viability assessment

The NIH 3T3 mouse embryonic fibroblast cells (ATCC) were used for the cell culture experiments for testing cytocompatibility of the composite. The cells were grown in 25 cm² culture flasks with DMEM, supplemented with 10% FBS and 1% antibiotic/antimycotic solution. Trypsinization of confluent cells in the culture flask was carried out using trypsin (0.25% trypsin–EDTA solution). The cells were counted using a hemocytometer (Improved Neubauer cell counter). Tissue culture polystyrene (TCPS) well plates were used as control in all the cell culture experiments.

The cellular viability after incubation of cells with different Fe complex concentration was quantified by MTT assay. In this assay, formazan crystals are formed when metabolically active cells react with MTT salt by the activity of oxidoreductase enzymes in the mitochondria. The concentration of the color formed by the formazan is directly proportional to the percentage of viable cells. Before adding MTT solution to the cell culture dishes, the cells were washed with PBS in order to remove any probe/complex present in the cell culture solution. Additionally, after incubation of cells with MTT solution, formed formazan crystals were dissolved in DMSO followed by centrifugation and OD was taken of the supernatant to avoid any interference during OD measurement. For MTT assay, 10 000 cells were seeded in each well of 96 well plate and incubated with Fe complex with various concentrations. After 24 h and 72 h of incubation, 0.5 mg mL^{-1} of the MTT solution was added to each well and incubated for a period of 2 h. The formazan crystals formed were later solubilized in DMSO and the optical density was recorded at 570 nm using an ELISA plate reader (Tecan InfiniteVR M1000 PRO). The MTT assay was repeated at least three times.

The cellular morphology and intracellular fluorescence after uptake of Fe complex were observed using fluorescence microscope (INCell Analyzer 6000, GE Healthcare Life Sciences, USA). The cells were grown in 24 well plate with Fe complex or ligand for 24 h and thereafter fixed with 3.7% formaldehyde in 1× PBS for 20 min and Hoechst 33258 dye was used to stain the nucleus of the cells. The cells were stained only using Hoechst 33258 dye which binds DNA of the cells and gives blue fluorescence. The fluorescence in green and red channels by cells is resulting in cellular uptake of the complex which is absent in the cells incubating without complex. All the experimental data, obtained using MTT assay are expressed as mean ± standard deviation (SD) and were analyzed by one-way ANOVA (SPSS 16.0) for the calculation of significance level of the experimental data. The differences were considered statistically significant, when $p \leq 0.05$.

3. Results and discussions

3.1 Selectivity study

The selectivity of **RG5NC** in MeCN solution was examined with different metal ions (like Al^{3+}, Ca^{2+}, Zn^{2+}, Cu^{2+}, Ni^{2+}, Cd^{2+}, Pb^{2+}, Fe^{3+}, Cr^{3+}, Hg^{2+} and Co^{2+}). As shown in Fig. 1a, after coordination of Fe^{3+} with **RG5NC**, the probe exhibited notably strong and high selective 'OFF–ON' absorption at $\lambda_{max} = 529$ nm. The free probe remained colorless when no Fe^{3+} ions were added into the solution. The solution color changed from colorless to orangish pink upon addition of Fe^{3+} ions into the **RG5NC** solution (inset Fig. 1b). Whereas, the other metal ions did not incite any visible color change. These results designates that **RG5NC** shows excellent selectivity for Fe^{3+} in MeCN solution.

To attain further thorough analysis on the selectivity of **RG5NC** for different metal ions, the change in the fluorescence intensity upon the addition of metal ions under the same condition was also examined by using fluorescence spectra. The fluorescence spectra of **RG5NC** in MeCN exhibited no fluorescence at 553 nm for free probe. Upon addition of Fe^{3+} to the **RG5NC** solution, a significant fluorescence enhancement was
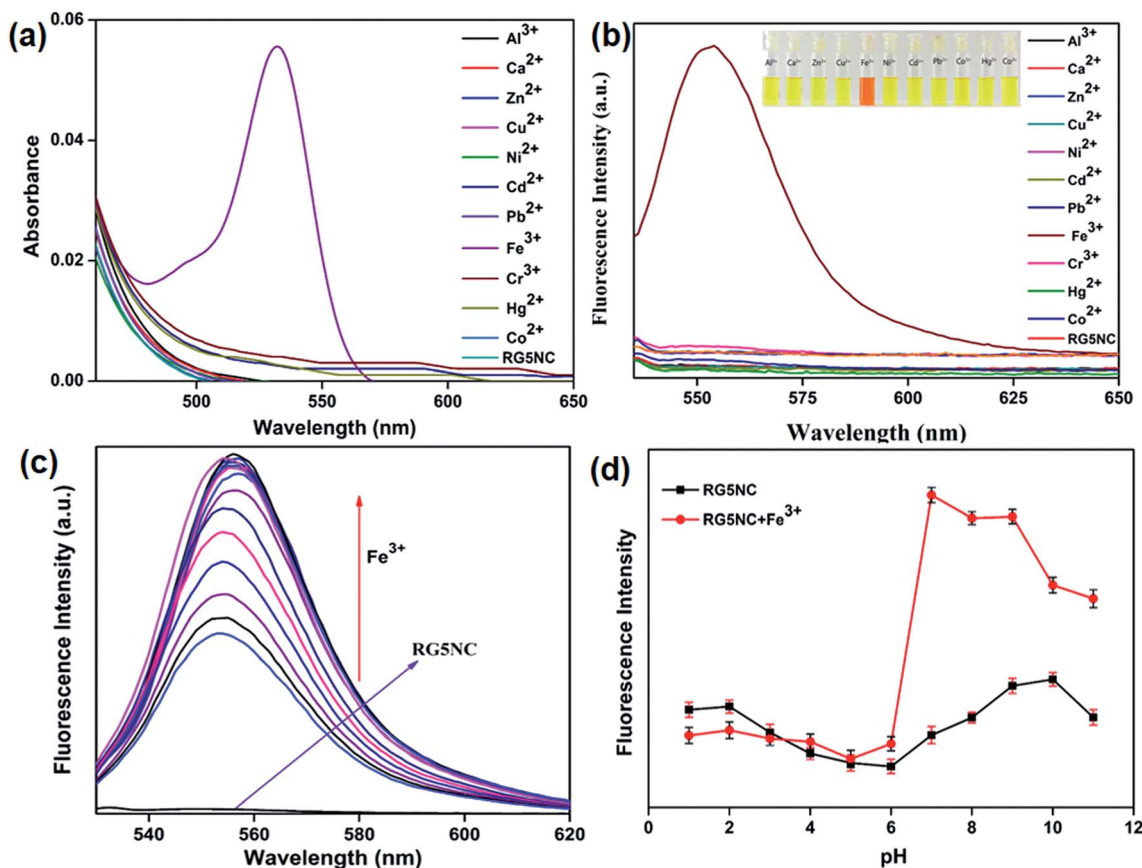
Fig. 1 (a) UV-vis spectra of **RG5NC** with different metal ions in MeCN. (b) Fluorescence spectra of **RG5NC** with different metal ions in MeCN solution. Inset: Picture depicting color change of **RG5NC** upon addition of various metal ions (c) fluorescence spectra of **RG5NC** for different concentrations of Fe^{3+} in MeCN solution. (d) Maximum fluorescence intensity of **RG5NC** at 553 nm in the absence and presence of Fe^{3+} at different pH.

observed as shown in Fig. 1b. All other metal ions did not display any fluorescence enhancement under similar conditions. These aspects indicate that opening of **RG5NC** spirolactam ring is due to the Fe^{3+} induced delocalization of xanthene moiety by chelation enhanced fluorescence (CHEF) mechanism and this reveal that **RG5NC** is a highly selective fluorescence chemosensor for Fe^{3+} and can be applied to biological sensing. The fluorescence quantum yield were calculated to be 2% and 78% in the absence and presence of Fe^{3+} ions (300 μM) respectively with rhodamine 6G as standard ($\Phi_F = 0.95$ in ethanol),.[29]

To gain more insight into the binding behavior of **RG5NC** with Fe^{3+}, fluorescence titrations of Fe^{3+} against **RG5NC** was monitored in MeCN solution. As seen in Fig. 1c, the free probe **RG5NC** did not show any fluorescence at 553 nm. Upon addition of Fe^{3+}, it leads to a remarkable increase in the emission intensities and reaches maximum at 300 μM. Since our main focus of the study was for sensing of biological samples and bio imaging it was necessary that the sensor is acceptable for physiological pH, hence, we evaluated the fluorescence response of **RG5NC** in presence and absence of Fe^{3+} at different pH values ranging from 1 to 11 as shown in Fig. 1d. The fluorescence OFF–ON worked well in the pH range 6 to 9, suggesting

that the sensor **RG5NC** could be easily used for determining Fe^{3+} in biological samples at physiological pH.

The limit of detection for this fluorescent probe was evaluated. Each spectrum was recorded at $\lambda_{ex/em} = 550/570$ nm. As shown in Fig. 2a, the Fe^{3+} concentration was varied over the range of 0.10–20 μM. The calculated detection limit of Fe^{3+} is 8.2×10^{-9} M with a good linear regression ($R = 0.992$).[30]

Further, binding constant of **RG5NC** with Fe^{3+} was calculated using a Benesi–Hildebrand plot.[31] The results in Fig. 2b shows a plot of $1/(I - I_0)$ versus $1/[Fe^{3+}]$ and yields a binding constant (K_a) value as 3.3×10^4 M^{-1} ($R^2 = 0.992$) suggesting the sensor binding ability between the probe and Fe^{3+} ion. The complexation ratio of **RG5NC** with Fe^{3+} was also explained in MeCN using Job's plot. The molar concentration of Fe^{3+} was varied from 0 to 0.9 in a solution containing $[Fe^{3+}] + [$**RG5NC**$]$ and the total concentration of **RG5NC** with Fe^{3+} was 20 μM. The obtained results suggests that the fluorescence intensity reached a maximum value when the molar fraction of Fe^{3+} is 0.5 (Fig. 2c), indicating that the Fe^{3+} complexes with **RG5NC** is in 1 : 1 binding ratio.

In order to further investigate the selectivity of **RG5NC** for Fe^{3+}, its selectivity for Fe^{3+} in presence of other competitive metal cations were examined under same conditions. Fig. 3a
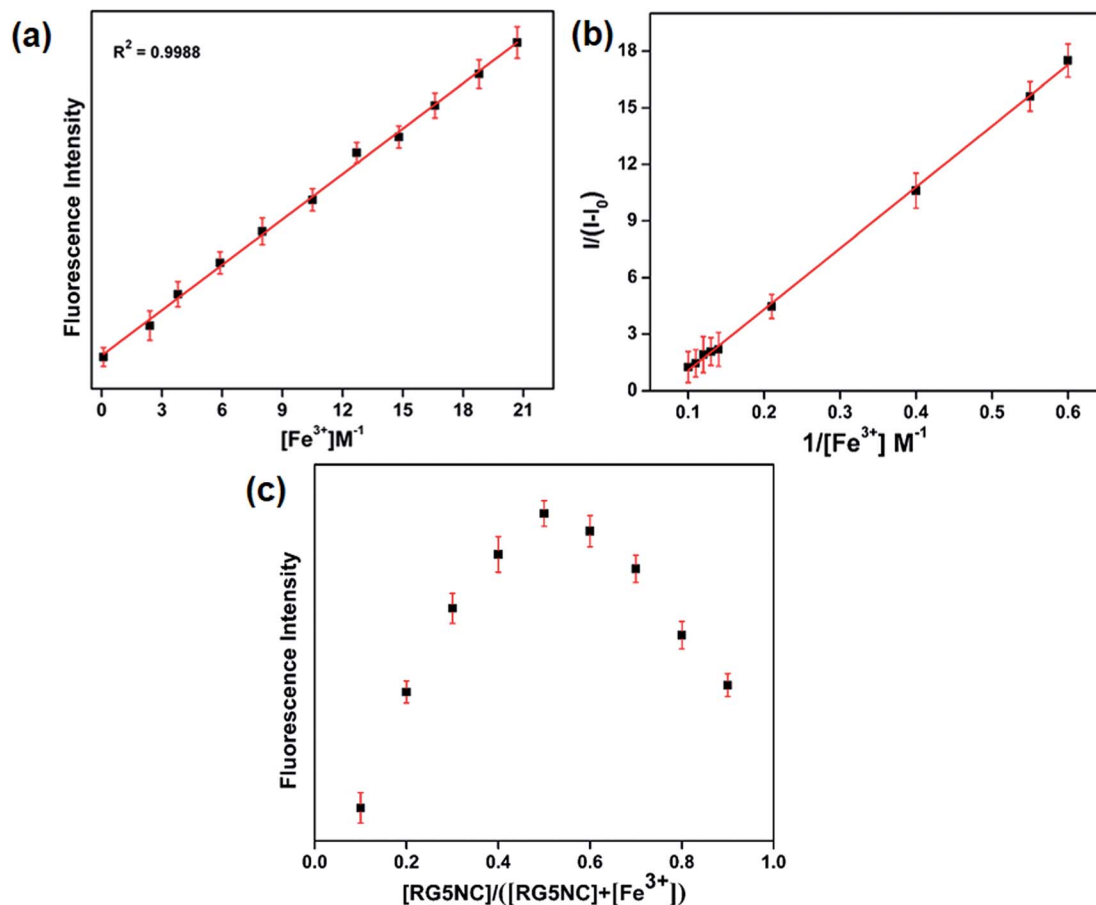
Fig. 2 (a) Fluorescence spectra of **RG5NC** with various concentration of Fe^{3+} in MeCN solution varying from 0–20 μM (b) Benesi−Hildebrand plot to evaluate binding constant. (c) Job's plot with a total concentration of [**RG5NC**] + [Fe^{3+}] = 20 μM.

depicts changes in the emission spectra of **RG5NC**. The detection was experimented in the presence/absence of other competitive metal cations. These results evidently indicates the noninterference of other competitive metal cations

during selective sensing of Fe^{3+}. One of the important parameters in developing a novel probe for practical and on field applications is its reversibility. The reversible interaction between **RG5NC** and Fe^{3+} was confirmed by the addition
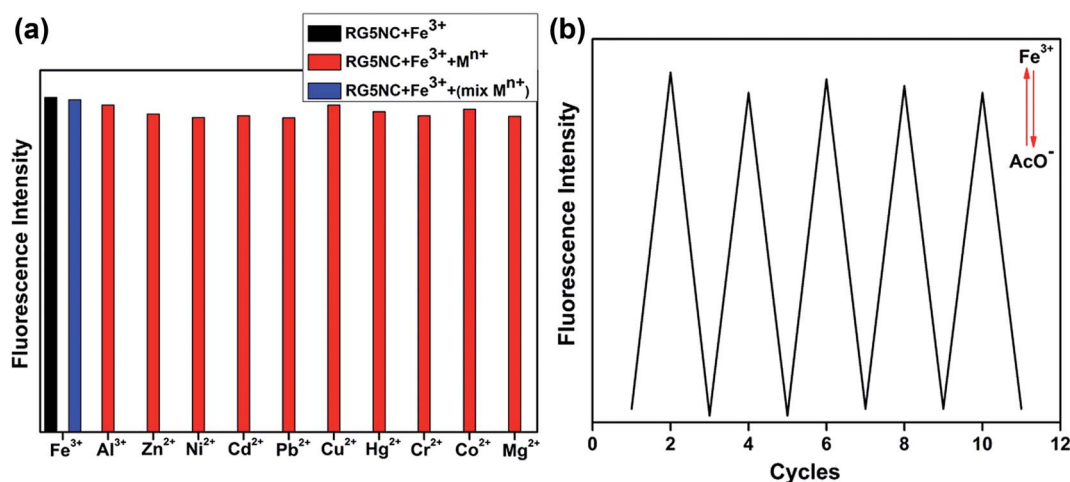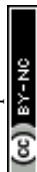

Fig. 3 (a) Selectivity of **RG5NC** for Fe^{3+} in presence of other metal cations. (b) Fluorescence spectra of **RG5NC** after sequential addition of Fe^{3+} and 1 : 1 AcO^- solution.
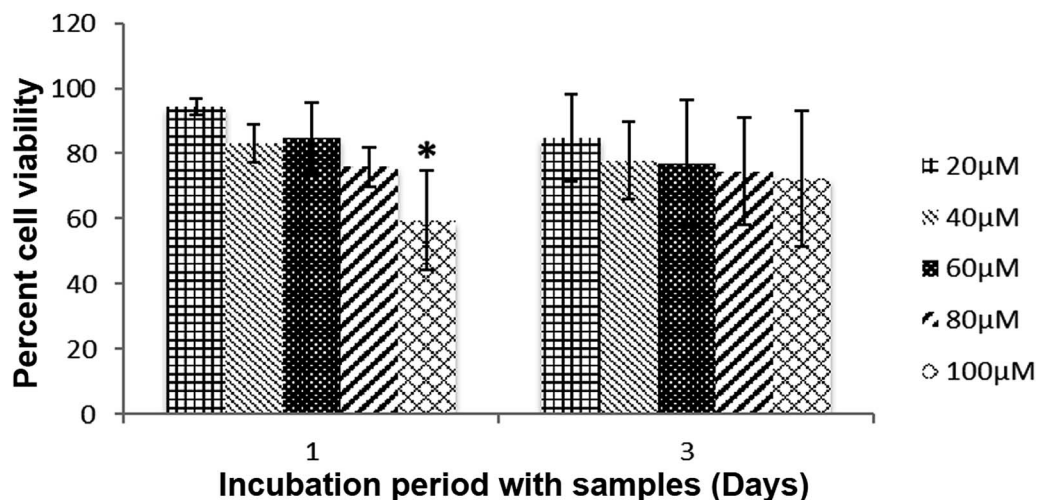
Fig. 4 NIH 3T3 cell viability grown with Fe complex. Error bars represent mean ± SD. Asterisk shows the significant difference at $p \leq 0.05$ with respect to control.

of AcO⁻ ions into the [**RG5NC–Fe³⁺**] complex. The experimental results exhibited color change from orangish red to colorless upon introduction of AcO⁻ ions forming iron acetate. Concurrently, about 95% of the fluorescence intensity was quenched. Then the fluorescence intensity was originally regained on addition of Fe^{3+} into the mixture. This process was repeated at least five times to suggest the reversibility of probe (Fig. 3b).

4. Cytocompatibility and cell imaging studies

The cytocompatibility of [**RG5NC–Fe³⁺**] complex was confirmed with NIH 3T3 cells *in vitro*. No significant difference was observed in the cell viability up to 80 μM concentration of [**RG5NC–Fe³⁺**] complex in the media (after 1 day of incubation) when compared to the control (Fig. 4). However,

at higher concentration (100 μM) the viability of cells was less compared to control. Interestingly, this difference in the viability disappeared when cells were allowed to grow with the [**RG5NC–Fe³⁺**] complex for 3 days. Initially, intracellular stress is induced because of higher concentration of [**RG5NC–Fe³⁺**] complex. However, with time, cells recover and start growing like control even at higher concentration of [**RG5NC–Fe³⁺**] complex.

The main aspect of the study was to detect the presence of Fe^{3+} in NIH 3T3 mouse embryonic fibroblast cells *in vitro*. Two different sets of cells, one were incubated with [**RG5NC–Fe³⁺**] and the other treated with just the probe. The latter set of cells did not show any fluorescence signal (Fig. 5) while the other exhibited fluorescence. Additionally the intensity of the signal was observed to increase with increase in concentration of the [**RG5NC–Fe³⁺**] uptake. The cells could efficiently uptake the probe and fluoresce illustrating its ability to act as sensor to detect Fe^{3+} *in vitro*.
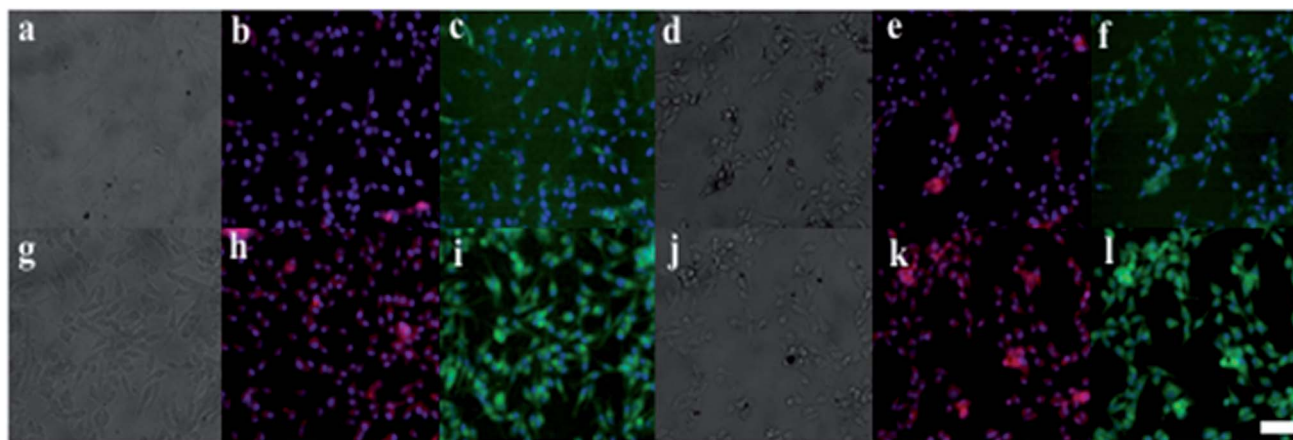

Fig. 5 Representative fluorescence images of NIH 3T3 cells after 24 h grown with 20 μM **RG5NC** (a) bright field, (b) red channel (c) green channel; 100 μM (d) bright field, (e) red channel (f) green channel; 20 μM [**RG5NC–Fe³⁺**] complex (g) bright field, (h) red channel (i) green channel and 100 μM Fe complex (j) bright field, (k) red channel (l) green channel. Scale bar is 50 μm.

4.1 Detection of Fe^{3+} in real samples

Further, we tested the applicability of this probe **RG5NC** for the detection of Fe^{3+} ions in real samples. We have used this probe to detect Fe^{3+} in industrial effluents, tap water, and Iron tablet (Irozorb) and Iron syrup (Orofex XT). In all the real samples significant fluorescence dependence on concentration was observed with a good liner response. Importantly, trace levels of metal ions could be detected using this probe **RG5NC** which ensured the potential analysis of Fe^{3+} in real sample sources. The obtained results were also validated by AAS and ICP-OES methods respectively. It is important to mention that testing of commercially available Iron syrup and Iron tablet for Fe^{3+} was examined using this probe. Each sample was analyzed with three of their replicates. The estimated detection limits have been tabulated in Table 1.

4.2 Response of RG5NC towards human blood serum

We have investigated the use of the probe towards the detection of Fe^{3+} ion in blood serum samples. In order to investigate the sensitivity of the probe **RG5NC** towards Fe^{3+} similar titration protocol was followed. Even in high serum condition the probe showed effective detection response towards Fe^{3+}. A linear change in the emission with good linear regression at 553 nm was observed. The control experiment was also performed to study the interaction of the probe **RG5NC** with human blood serum under similar conditions. The obtained values detected from this method matched well with the mM values of Fe^{3+} ion given in certified reference material (CRM). The results were also validated by AAS and ICP-OES methods respectively. The experiments
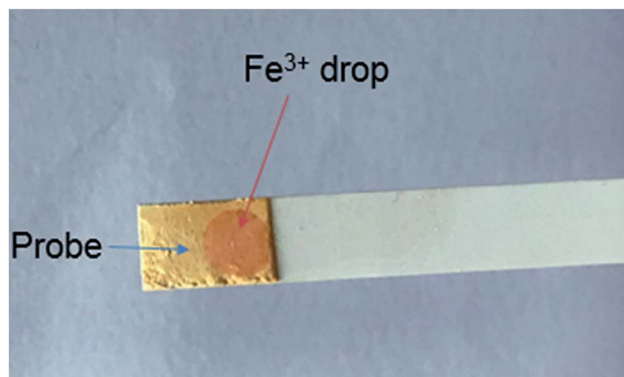

Fig. 6 Photograph of the test strip of this probe **RG5NC** during the detection of Fe^{3+}.

were conducted in triplicates. The determined Fe^{3+} content in human blood samples have been tabulated in Table 2.

5. Fast track detection of Fe^{3+} using test strips

Assuring purity of drinking water and consumable food materials in remote areas is a challenging task where laboratory facilities are not available. Hence portable test strips were prepared for quick on-filed detection of Fe^{3+} ions. For this purpose test strips were soaked in MeCN solution of **RG5NC** and then dried in air before they were used for detection of Fe^{3+} in water. A distinct color change was observed immediately upon dipping the test strips in Fe^{3+} ion solution (Fig. 6). Presence of Fe^{3+} selectively changed the test-strips color to orangish

Table 1 Determination of Fe^{3+} in real samples

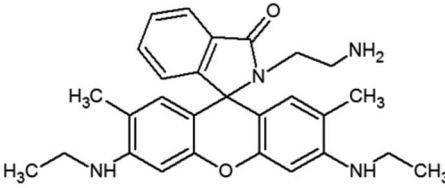| Samples	Fe^{3+} found by AAS method (M)	RSD (%)	Fe^{3+} found by present method (M)	SE
Iron syrup	9.12×10^{-5}	2.24	6.08×10^{-5}	2.11
Iron tablet	1.16×10^{-4}	2.10	1.05×10^{-5}	1.91
Industrial effluent1	8.38×10^{-4}	2.81	7.50×10^{-4}	1.17
Industrial effluent2	6.24×10^{-4}	1.62	6.28×10^{-4}	1.53
Tap water	2.21×10^{-4}	2.54	1.55×10^{-4}	2.76
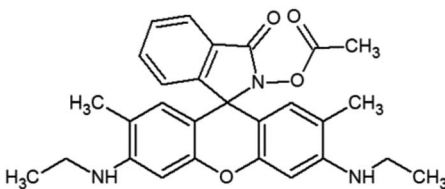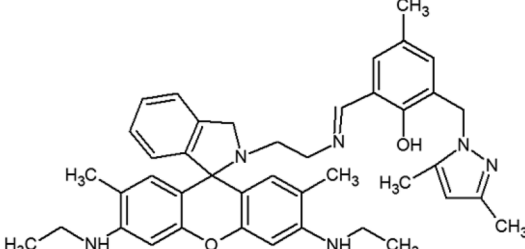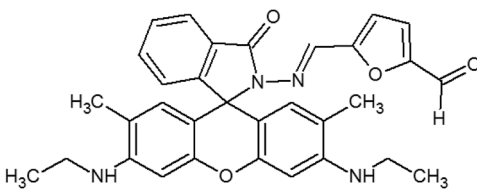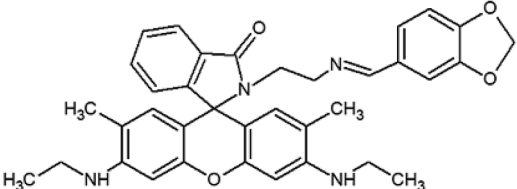
Table 2 Determination of Fe^{3+} in various human blood serum samples using **RG5NC**[a]

Samples	Fe^{3+} found by ICP_OES method (M)	RSD (%)	Fe^{3+} found by present method (M)	SE
CBRM1	5.96×10^{-2}	3.64	5.67×10^{-2}	1.81
CBRM2	5.94×10^{-2}	1.70	5.63×10^{-2}	1.23
CBRM3	5.92×10^{-2}	2.02	5.62×10^{-2}	1.57
BS1	5.99×10^{-2}	1.94	5.87×10^{-2}	0.76
BS2	6.01×10^{-2}	1.17	5.83×10^{-2}	0.95
BS3	6.05×10^{-2}	1.63	5.85×10^{-2}	1.84

[a] CBRM: certified blood reference material, BS: blood serum samples.

Table 3 Comparison of our probe performance with various other reported probes

Probe	Detection limit	Reference
(chemical structure)	1.42×10^{-6} M	32a
(chemical structure)	0.03×10^{-6} M	32b
(chemical structure)	0.29×10^{-6} M	32c
(chemical structure)	17×10^{-9} M	32d
(chemical structure)	1.18×10^{-8} M	32e
Present work	8.2×10^{-9} M	—

red. This newly developed sensor system provide an alternative method to confirm the nature as well as the extent of metal ion induced toxicity in natural water sources.

A comparison of the applicability and analytical section of this probe with some of the previous reports in terms of their solubility and detection limit[32] is shown in Table 3.

6. Conclusion

The synthesized probe showed an outstanding sensitivity and selectivity for Fe^{3+} in human blood serum samples and excellent uptake by cells for imaging applications. The detection limit was about 8.2 nM. Spectral changes were observed to be reversible with respect to spirolactam ring opening. Confocal laser scanning microscopy experiments showed that **RG5NC** could be used to detect Fe^{3+} in live cells. The probe sensitivity of metal ion recognition was investigated in human blood serum. The detection as well as the discrimination of this toxic metal ion was also achieved in real samples at nano molar level. In addition we have also demonstrated this detection of Fe^{3+} ions using portable test strips. The significance of this study lies in applying such fluorescent probes for rapid on field detection of Fe^{3+} in human blood serum and live cells.

Conflicts of interest

There are no conflicts to declare.

Acknowledgements

References

1 Y. Liu, R. Shen, J. Ru, X. Yao, Y. Yang, H. Liu, X. Tanga, D. Bai, G. Zhang and W. Liu, A reversible rhodamine 6G-based fluorescence turn-on probe for Fe^{3+} in water and its application in living cells imaging, *RSC Adv.*, 2016, **6**(113), 111754–111759.

2 C. Wang, Y. Huang, K. Jiang, M. G. Humphrey and C. Zhang, Dual-emitting quantum dots/carbon nanodots-based nanoprobe for selective and sensitive detection of Fe^{3+} in cells, *Analyst*, 2016, (2013), 1–3.

3 S. Hu, S. Zhang, C. Gao, C. Xu and Q. Gao, A new selective fluorescent sensor for Fe^{3+} based on a pyrazoline derivative, *Spectrochim. Acta, Part A*, 2013, **113**(2013), 325–331.

4 (a) X. Qu, Q. Liu, X. Ji, H. Chen, Z. Zhou and Z. Shen, Enhancing the Stokes' shift of BODIPY dyes via through-bond energy transfer and its application for Fe^{3+}-detection in live cell imaging, *Chem. Commun.*, 2012, **48**(2012), 4600–4602; (b) Y. Guo, F. Cao and Y. Li, Solid phase synthesis of nitrogen and phosphor co-doped carbon quantum dots for sensing Fe^{3+} and the enhanced photocatalytic degradation of dyes, *Sens. Actuators, B*, 2017, 1105–1111.

5 Q. Yang, W. Lin, X. Zheng and L. Xiao, Single Particle Dynamic Imaging and Fe^{3+} Sensing with Bright Carbon Dots Derived from Bovine Serum Albumin Proteins, *Sci. Rep.*, 2015, **5**, 17727.

6 (a) H. R. Chandan and B. R. Geetha, Study on precipitation efficiency of solvents in postpreparative treatment of nanocrystals, *J. Mater. Res.*, 2013, **28**(21), 3003–3009; (b) H. R. Chandan, M. Venkataramana, M. D. Kurkuri and R. G. Balakrishna, Simple quantum dot bioprobe/label for sensitive detection of Staphylococcus aureus TNase, *Sens. Actuators, B*, 2016, **222**, 1201–1208.

7 H. Chandan, V. Saravanan, R. K. Pai and R. G. Balakrishna, Synergistic effect of binary ligands on nucleation and growth/size effect of nanocrystals: Studies on reusability of the solvent, *J. Mater. Res.*, 2014, **29**(14), 1556–1564.

8 L. P. D'Souza, V. Amoli, H. R. Chandan, A. K. Sinha, R. Krishna Pai and G. R. Balakrishna, Atomic force microscopic study of nanoscale interaction between N719 dye and CdSe quantum dot in hybrid solar cells and their enhanced open circuit potential, *Sol. Energy*, 2015, **116**, 25–36.

9 R. M. Renuka, J. Achuth, H. R. Chandan, M. Venkataramana and K. Kadirvelu, A fluorescent dual aptasensor for the rapid and sensitive onsite detection of E. coli O157:H7 and its validation in various food matrices, *New J. Chem.*, 2018, **42**(13), 10807–10817.

10 H. R. Chandan, J. D. Schiffman and R. G. Balakrishna, Quantum dots as fluorescent probes: Synthesis, surface chemistry, energy transfer mechanisms, and applications, *Sens. Actuators, B*, 2018, **258**, 1191–1214.

11 C. Hunsur Ravikumar, M. Ira Gowda and R. G. Balakrishna, An "OFF–ON" quantum dot–graphene oxide bioprobe for sensitive detection of micrococcal nuclease of Staphylococcus aureus, *Analyst*, 2019, 3999–4005.

12 X. Pu, B. Hu, Z. Jiang and C. Huang, Speciation of dissolved iron(II) and iron(III) in environmental water samples by gallic acid-modified nanometer-sized alumina micro-column separation and ICP-MS determination, *Analyst*, 2005, **130**(8), 1175–1181.

13 N. Mir, P. Karimi, C. E. Castano, N. Norouzi, J. V. Rojas and R. M., Functionalizing $Fe_3O_4@SiO_2$ with a novel mercaptobenzothiazole derivative: Application to trace fluorometric and colorimetric detection of Fe^{3+} in water, *Appl. Surf. Sci.*, 2019, 876–888.

14 Z. Zuo, X. Song, D. Guo, Z. Guo and Q. Niu, A dual responsive colorimetric/fluorescent turn-on sensor for highly selective, sensitive and fast detection of Fe^{3+} ions and its applications, *J. Photochem. Photobiol., B*, 2019, 111876.

15 H. Y. Lee, D. R. Bae, J. C. Park, H. Song, W. S. Han and J. H. Jung, A Selective Fluoroionophore Based on BODIPY-functionalized Magnetic Silica Nanoparticles: Removal of Pb^{2+} from Human Blood, *Angew. Chem., Int. Ed.*, 2009, **48**(2009), 1239–1243.

16 M. Park, S. Seo, S. J. Lee and J. H. Jung, Functionalized $Ni@SiO_2$ core/shell magnetic nanoparticles as a chemosensor and adsorbent for Cu^{2+} ion in drinking water and human blood, *Analyst*, 2010, **135**(2010), 2802–2805.

17 L. Liu, X. Dong, Y. Xiao, W. Lian and Z. Liu, Two-photon excited fluorescent chemosensor for homogeneous determination of copper(II) in aqueous media and complicated biological matrix, *Analyst*, 2011, **136**(2011), 2139–2145.

18 J. Hatai, S. Pal and S. Bandyopadhyay, An inorganic phosphate (Pi) sensor triggers 'turn-on' fluorescence response by removal of a Cu^{2+} ion from a Cu^{2+}-ligand sensor: determination of Pi in biological samples, *Tetrahedron Lett.*, 2012, **53**(2012), 4357–4360.

19 V. V. Halali, M. Saxena, H. R. Chandan, A. A. Ojha and R. G. Balakrishna, Paper based field deployable sensor for naked eye monitoring of copper(II) ions; elucidation of binding mechanism by DFT studies, *Spectrochim. Acta, Part A*, 2019, (2019), 117291.

20 J. Li, Q. Wang, Z. Guo, H. Ma, Y. Zhang, B. Wang, D. Bin and Q. Wei, Highly selective fluorescent chemosensor for detection of Fe^{3+} based on $Fe_3O_4@ZnO$, *Sci. Rep.*, 2016, **6**, 23558.

21 (a) L. Yang, W. Zhu, M. Fang, Q. Zhang and C. Li, A new carbazole-based Schiff-base as fluorescent chemosensor for selective detection of Fe^{3+} and Cu^{2+}, *Spectrochim. Acta, Part A*, 2013, **109**(2013), 186–192; (b) V. K. Gupta, N. Mergu and L. K. Kumawat, A new multifunctional rhodamine-derived probe for colorimetric sensing of Cu(II) and Al(III) and

fluorometric sensing of Fe(III) in aqueous media, *Sens. Actuators, B*, 2016, **223**(2016), 101–113.

22 (*a*) S. Ma, Z. Yang, M. She, W. Sun, B. Yin, P. Liu, S. Zhang and J. Li, Design and synthesis of functionalized rhodamine based probes for specific intracellular fluorescence imaging of Fe^{3+}, *Dyes Pigm.*, 2015, **115**(2015), 120–126; (*b*) F. Yan, T. Zheng, D. Shi, Y. Zou, Y. Wang, M. Fu, L. Chen and W. Fu, Rhodamine-aminopyridine based fluorescent sensors for Fe^{3+} in water: Synthesis, quantum chemical interpretation and living cell application, *Sens. Actuators, B*, 2015, **215**(2015), 598–606; (*c*) M. S. Moorthy, H.-B. Kim, A.-R. Sung, J.-H. Bae, S.-H. Kim and C.-S. Ha, Fluorescent mesoporous organosilicas for selective monitoring of Hg^{2+} and Fe^{3+} ions in water and living cells, *Microporous Mesoporous Mater.*, 2014, **194**(2014), 219–228; (*d*) Y.-H. He, J.-P. Lai, S. Hui, Z.-M. Chen and S. Lan, A fast, sensitive and stable fluorescent fiber-optic chemosensor for quantitative detection of Fe^{3+} in real water and HepG2 living cells, *Sens. Actuators, B*, 2015, **225**(2016), 405–412; (*e*) C.-Y. Li, C.-X. Zou, Y.-F. Li, J.-L. Tang and C. Weng, A new rhodamine-based fluorescent chemosensor for Fe^{3+} and its application in living cell imaging, *Dyes Pigm.*, 2014, **104**(2014), 110–115; (*f*) S. Chan, Q. Li, H. Tse, A. W. M. Lee, N. K. Mak, H. L. Lung and W.-H. Chan, Rhodamine-based "off–on" fluorescent chemosensor for selective detection of Fe^{3+} in aqueous media and its application in bioimaging, *RSC Adv.*, 2016, 74389–74393; (*g*) X. Jin, S. Wang, W. Yin, T. Xu, J. Yang, L. Qi, X. Xia and J. Liu, A highly sensitive and selective fluorescence chemosensor for Fe^{3+} based on rhodamine and its application *in vivo* imaging, *Sens. Actuators, B*, 2017, **247**(2017), 461–468; (*h*) F. Zhou, T.-H. Leng, Y.-J. Liu, C.-Y. Wang, P. Shi and W.-H. Zhu, Water-soluble rhodamine-based chemosensor for Fe^{3+} with high sensitivity, selectivity and anti-interference capacity and its imaging application in living cells, *Dyes Pigm.*, 2017, 429–436; (*i*) S. Adhikari, A. Ghosh, M. Ghosh and D. D. Subhajit Guria, Ratiometric sensing of Fe^{3+} through PET-CHEF-FRET processes: live cell imaging, speciation and DFT studies, *Sens. Actuators, B*, 2017, 942–950; (*j*) S. K. Dwivedi, R. C. Gupta, R. Ali, S. S. Razi, S. K. H., P. P. Manna and A. Misra, Smart PET based organic scaffold exhibiting bright "Turn-On" green fluorescence to detect Fe^{3+} ion: Live cell imaging and logic implication, *J. Photochem. Photobiol., B*, 2018, 157–166; (*k*) B. Lim, B. Baek, K. Jang, N. K. Lee, J. H. Lee, Y. Lee, J. Kim, S. W. Kang, J. Park, S. Kim, N.-W. Kang, S. Hong, D.-D. Kim, I. Kim, H. Hwang and J. Lee, Novel turn-on fluorescent biosensors for selective detection of cellular Fe^{3+} in lysosomes: Thiophene as a selectivity-tuning handle for Fe^{3+} sensors, *Dyes Pigm.*, 2019, 51–59; (*l*) W. Wang, M. Wu, H. Liu, Q. Liu, Y. Gao and B. Zhao, A novel on–off–on fluorescent chemosensor for relay detection of Fe^{3+} and PPi in aqueous solution and living cells, *Tetrahedron Lett.*, 2019, 1631–1635; (*m*) X. Gong, H. Zhang, N. Jiang, L. Wang and G. Wang, Oxadiazole-based 'on-off' fluorescence chemosensor for rapid recognition and detection of Fe^{2+}

and Fe^{3+} in aqueous solution and in living cells, *Microchem. J.*, 2019, **145**(2019), 435–443.

23 (*a*) D. T. Quang and J. S. Kim, Fluoro- and Chromogenic Chemodosimeters for Heavy Metal Ion Detection in Solution and Biospecimens, *Chem. Rev.*, 2010, **110**(10), 6280–6301; (*b*) Y. Yang, Q. Zhao, W. Feng and F. Li, Luminescent Chemodosimeters for Bioimaging, *Chem. Rev.*, 2013, **113**(1), 192–270.

24 (*a*) V. K. G. Kumar, N. Mergu and A. Singh, Rhodamine-derived highly sensitive and selective colorimetric and off–on optical chemosensors for Cr^{3+}, *Sens. Actuators, B*, 2015, **220**(2015), 420–432; (*b*) S. Sun, B. Qiao, N. Jiang, J. Wang, S. Zhang and X. Peng, Naphthylamine–Rhodamine-Based Ratiometric Fluorescent Probe for the Determination of Pd^{2+} Ions, *Org. Lett.*, 2013, 1132–1135; (*c*) S.-K. Ko, Y.-K. Yang, J. Tae and I. Shin, *In Vivo* Monitoring of Mercury Ions Using a Rhodamine-Based Molecular Probe, *J. Am. Chem. Soc.*, 2006, **128**(2006), 14150–14155; (*d*) F. Ge, H. Ye, H. Zhang and B.-X. Zhao, A novel ratiometric probe based on rhodamine B and coumarin for selective recognition of Fe(III) in aqueous solution, *Dyes Pigm.*, 2013, **99**, 661–665; (*e*) X. Li, Y. Yin, J. Deng, H. Zhong, J. Tang, Z. Chen, L. Yang and L.-J. Ma, A solvent-dependent fluorescent detection method for Fe^{3+} and Hg^{2+} based on a rhodamine B derivative, *Talanta*, 2016, **154**, 329–334; (*f*) W. Yin, H. Cui, Z. Yang, C. Li, M. She, B. Yin, J. Li, G. Zhao and Z. Shi, Facile synthesis and characterization of rhodamine-based colorimetric and "off–on" fluorescent chemosensor for Fe^{3+}, *Sens. Actuators, B*, 2011, **157**(2), 675–680; (*g*) M. Chai, M. Li, D. Zhang, C.-c. Wang, Y. Ye and Y. Zhao, Three colorimetric and off–on fluorescent chemosensors for Fe^{3+} in aqueous media, *Luminescence*, 2013, **28**(4), 557–561; (*h*) X. Han, D.-E. Wang, S. Chen, L. Zhang, Y. Guo and J. Wang, A new rhodamine-based chemosensor for turn-on fluorescent detection of Fe^{3+}, *Anal. Methods*, 2015, **7**(10), 4231–4236.

25 (*a*) B. Rathinam, C.-C. Chien, B.-C. Chen and J.-H. Liu, Fluorogenic and chromogenic detection of Cu^{2+} and Fe^{3+} species in aqueous media by rhodamine–triazole conjugate, *Tetrahedron*, 2013, **69**(1), 235–241; (*b*) T. Geng, R. Huang and D. Wu, Turn-on fluorogenic and chromogenic detection of Fe^{3+} and Cr^{3+} in a completely water medium with polyacrylamide covalently bonding to rhodamine B using diethylenetriamine as a linker, *RSC Adv.*, 2014, **4**(86), 46332–46339; (*c*) L. K. Kumawat, N. Mergu, M. Asif and V. K. Gupta, Novel synthesized antipyrine derivative based "Naked eye" colorimetric chemosensors for Al^{3+} and Cr^{3+}, *Sens. Actuators, B*, 2016, **231**, 847–859.

26 B. Rathinam, C. C. Chien, B.-C. Chen and J.-H. Liu, Fluorogenic and chromogenic detection of Cu^{2+} and Fe^{3+} species in aqueous media by rhodamineetriazole conjugate, *Tetrahedron*, 2013, **69**(2013), 235–241.

27 (*a*) N. R. Chereddy, K. Suman, P. S. Korrapati, S. Thennarasu and A. B. Mandal, Design and synthesis of rhodamine based chemosensors for the detection of Fe^{3+} ions, *Dyes Pigm.*, 2012, **95**(3), 606–613; (*b*) C.-Y. Li, C.-X. Zou, Y.-F. Li,

J.-L. Tang and C. Weng, A new rhodamine-based fluorescent chemosensor for Fe^{3+} and its application in living cell imaging, *Dyes Pigm.*, 2014, **104**, 110–115.

28 (*a*) T. R. Mahalingam, S. Vijayalakshmi, R. K. Prabhu, A. Thiruvengadasami, C. K. Mathews and K. R. Shanmugasundaram, Studies on some trace and minor elements in blood. A survey of the Kalpakkam (India) population. Part I: Standardization of analytical methods using ICP-MS and AAS, *Biol. Trace Elem. Res.*, 1997, **57**(3), 191–206; (*b*) N. B. Ivanenko, A. A. Ganeev, N. D. Solovyev and L. N. Moskvin, Determination of Trace Elements in Biological Fluids, *J. Anal. Chem.*, 2011, 900–915; (*c*) T. R. Mahalingam, S. Vijayalakshmi, R. Krishna Prabhu, A. Thiruvengadasami, A. Wilber, C. K. Mathews and K. R. Shanmugasundaram, Studies on Some Trace and Minor Elements in Blood, *Biol. Trace Elem. Res.*, 1996.

29 K.-P. Wang, J.-P. Chen, S.-J. Zhang, Y. Lei, H. Zhong, S. Chen, X.-H. Zhou and Z.-Q. Hu, Thiophene-based rhodamine as selective fluorescence probe for Fe(III) and Al(III) in living cells, *Anal. Bioanal. Chem.*, 2017, **409**(23), 5547–5554.

30 H. L. Yan Gao, Q. Liu and W. Wang, A novel colorimetric and OFF–ON fluorescent chemosensor based on fluorescein derivative for the detection of Fe^{3+} in aqueous solution and living cells, *Tetrahedron Lett.*, 2016, 1852–1855.

31 Y. Liu, R. Shen, J. Ru, X. Yao, Y. Yang, H. Liu, X. Tang, D. Bai, G. Zhang and W. Liu, A reversible rhodamine 6G-based fluorescence turn-on probe for Fe^{3+} in water and its application in living cell imaging, *RSC Adv.*, 2016, 111754–111759.

32 (*a*) Z.-Q. Hu, Y.-Y. Gu, W.-Z. Hu, L.-L. Sun, J.-H. Zhu and Y. Jiang, A Highly Selective and Sensitive Turn-On Fluorescent Chemosensor Based on Rhodamine 6G for Iron(III), *ChemistryOpen*, 2014, **3**(6), 264–268; (*b*) B. Wang, J. Hai, Z. Liu, Q. Wang, Z. Yang and S. Sun, Selective Detection of Iron(III) by Rhodamine-Modified Fe_3O_4 Nanoparticles, *Angew. Chem., Int. Ed.*, 2010, 4576–4579; (*c*) R. Alam, R. Bhowmick, A. S. M. Islam, A. katarkar, K. Chaudhuri and M. Ali, A rhodamine based fluorescent trivalent sensor (Fe^{3+},Al^{3+},Cr^{3+}) with potential applications for a live cell imaging and combinatorial logic circuit and memory device, *New J. Chem.*, 2017, **41**, 8359–8369; (*d*) A. Kumar, C. Kumari, D. Sain, S. K. Hira, P. P. Manna and S. Dey, Synthesis of Rhodamine-Based Chemosensor for Fe^{3+} Selective Detection with off–on Mechanism and its Biological Application in DL-Tumor Cells, *ChemistrySelect*, 2017, **2**(2017), 2969–2974; (*e*) W. Sun, X. Cao, F. Zhang, Y. Bai and X. Ding, A Highly Selective "Turn-on" Fluorescent Probe for Detection of Fe^{3+} in Cells, *J. Fluoresc.*, 2019, 425–434.